arXiv:1201.1176v2 [cond-mat.quant-gas] 24 Apr 2012

Origin of the Three-body Parameter Universality in Efimov Physics

Jia Wang,[1] J. P. D'Incao,[1] B. D. Esry,[2] and Chris H. Greene[1]
[1]*Department of Physics and JILA, University of Colorado, Boulder, CO 80309-0440*
[2]*Department of Physics, Kansas State University, Manhattan, Kansas 66506, USA*

In recent years extensive theoretical and experimental studies of universal few-body physics have led to advances in our understanding of universal Efimov physics. Whereas theory had been the driving force behind our understanding of Efimov physics for decades, recent experiments have contributed an unexpected discovery. Specifically, measurements have found that the so-called *three-body parameter* determining several properties of the system is universal, even though fundamental assumptions in the theory of the Efimov effect suggest that it should be a variable property that depends on the precise details of the short-range two- and three-body interactions. The present Letter resolves this apparent contradiction by elucidating previously unanticipated implications of the two-body interactions. Our study shows that the three-body parameter universality emerges because a universal effective barrier in the three-body potentials prevents the three particles from simultaneously getting close together. Our results also show limitations on this universality, as it is more likely to occur for neutral atoms and less likely to extend to light nuclei.

PACS numbers: 31.15.ac,31.15.xj,67.85.-d

In the early 70's, Vitaly Efimov predicted a strikingly counterintuitive quantum phenomenon [1], today known as Efimov effect: in three-body systems for which the two-body s-wave scattering length a is much larger than the characteristic range r_0 of the two-body interaction, an infinite number of three-body bound states can be formed even when the short-range two-body interactions are too weak to bind a two-body state ($a < 0$). The Efimov effect, once considered a mysterious and esoteric effect, is today a reality that many experiments in ultracold quantum gases have successfully observed and continued to explore [2–14]. One of the most fundamental assumptions underlying our theoretical understanding of this peculiar effect is that the weakly bound three-body energy spectrum, and other low-energy three-body scattering observables, should depend on a three-body parameter that encapsulates all details of the interactions at short distances [15]. For this reason, the three-body parameter has been viewed as nonuniversal since its value for any specific system would depend on the precise details of the underlying two- and three-body interactions [16–18].

In nuclear physics, this picture seems be consistent, i.e., three-body weakly bound state properties seem to be sensitive to the nature of the two- and three-body short-range interactions [17]. More recently, however, Berninger *et al.* [3] have directly explored this issue for alkali atoms whose scattering lengths are magnetically tuned near different Fano-Feshbach resonances [19]. Even though the short-range physics can be expected to vary from one resonance to another, Efimov resonances were found for values of the magnetic field at which $a{=}a^-_{3\mathrm{b}}{=}{-}9.1(2)r_{\mathrm{vdW}}$, where r_{vdW} is the van der Waals length [20, 21]. Therefore, in each of these cases, the three-body parameter was approximately the same, thus challenging a fundamental assumption of the universal theory. Even more striking is the observation that the Efimov resonance positions obtained for ^{39}K [4], ^{7}Li [5–7], ^{6}Li [8–11], and ^{85}Rb [12] are also consistent with values of $a^-_{3\mathrm{b}}/r_{\mathrm{vdW}}$ found for ^{133}Cs [3]. (Note that the work in Ref. [7] also provided early suggestive evidence of such universal behavior.) These observations provide strong evidence that the three-body parameter has universal character for spherically-symmetric neutral atoms, and therefore suggest that *something else* beyond the universal theory needs to be understood.

In this Letter, we identify precisely the physics beyond the universal theory needed to explain a universal three-body parameter, presenting theoretical evidence to support the recent experimental observations. Previous work has shown that the three-body parameter can be universal — that is, independent of the details of the interactions — in three-polar-molecule systems [22] and in three-atom systems near narrow Fano-Feshbach resonance [23, 24], although recent work has shown that the latter case likely requires even more finely-tuned conditions [25]. Our present numerical analysis, however, adds another, broader class of systems with a universal three-body parameter: systems with two-body interactions that efficiently suppress the probability to find any pair of particles separated by less than r_0 (see Section A in Ref. [26]). This class of systems, therefore, is more closely related to systems near broad Fano-Feshbach resonances [19].

Such a suppression could derive from the usual classical suppression of the probability for two particles to exist between r and $r + dr$ in regions of high *local* velocity $\hbar k_L(r)$, which is proportional to $[\hbar k_L(r)/mdr]^{-1}$ (m being the particle mass), the time spent in that interval dr (see Section B in Ref. [26]). It is possible that there could be an additional suppression as well, through quantum reflection from a potential *cliff* [27]. Systems supporting many bound states, such as the neutral atoms used in ultracold experiments with their strong van der Waals attraction, clearly exhibit this suppression. In general, a finite-range two-body potential that supports many

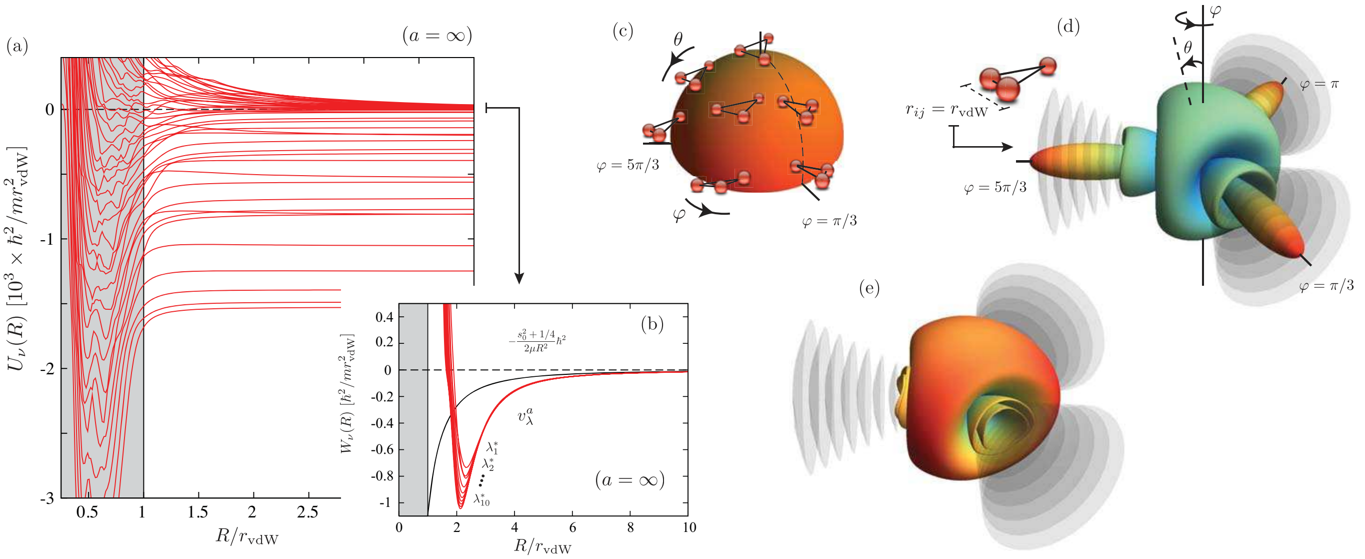

FIG. 1: (a) The full energy landscape for the three-body potentials at $a=\infty$ for our v_λ^a model potential supporting 25 two-body bound states. (b) effective diabatic potentials W_ν relevant for Efimov physics for v_λ^a with an increasingly large number of bound states (λ_n^* is the value of λ that produces $a=\infty$ and n s-wave bound states). W_ν converge to a universal potential displaying the repulsive barrier at $R\approx 2r_{\rm vdW}$ that prevents particles access to short distances. (c)-(e) demonstrate the suppression of the wave function inside the potential well through the channel functions $\Phi_\nu(R;\theta,\varphi)$ for R fixed near the minima of the Efimov potentials in (b). (c) shows the mapping of the geometrical configurations onto the hyperangles θ and φ. (d) and (e) show the channel functions, where the "distance" from the origin determines $|\Phi_\nu|^{1/2}$, for two distinct cases: in (d) when there is a substantial probability to find two particles inside the potential well (defined by the region containing the gray disks) and in (e) with a reduced probability — see also our discussion in Fig. 2. In (d) and (e), we used the potentials $v_{\rm sch}$ and v_λ^a, respectively, both with $n=3$. Note that we have used $\Phi_\nu(R;\theta,\varphi)=\Phi_\nu(R;\pi-\theta,\varphi)$ to generate the lower half of the surface plots.

bound states decreases steeply with decreasing interparticle distance r, starting when $r/r_{\rm vdW}\lesssim 1$, at which point the potential cliff plays a role analogous to a repulsive potential for low-energy scattering. We demonstrate this fact by showing that the three-body parameter in the presence of many two-body bound states roughly coincides with that for a 100% reflective two-body model potential, where the two-body short-range potential well is replaced by a hard-sphere.

The starting point for our investigation of the universality of the three-body parameter is the adiabatic hyperspherical representation [18, 28]. This representation offers a simple and conceptually clear description by reducing the problem to the solution of the "hyperradial" Schrödinger equation :

$$\left[-\frac{\hbar^2}{2\mu}\frac{d^2}{dR^2}+W_\nu(R)\right]F_\nu(R) + \sum_{\nu'\neq\nu} W_{\nu\nu'}(R)F_{\nu'}(R) = EF_\nu(R). \quad (1)$$

Here, the hyperradius R describes the overall size of the system; ν is the channel index; $\mu=m/\sqrt{3}$ is the three-body reduced mass for particle masses m; E is the total energy; and F_ν is the hyperradial wave function. The nonadiabatic couplings $W_{\nu\nu'}$ drive inelastic transitions, and the effective hyperradial potentials W_ν support bound and resonant states. To treat problems with deep two-body interactions — necessary to see strong inside-the-well suppression — requires us to solve Eq. (1) for two-body model interactions that support many bound states, a challenge for most theoretical approaches. Using our recently developed methodology [29], however, we were able to treat systems with up to 100 two-body ro-vibrational bound states and solve Eq. (1) beyond the adiabatic approximation. Here, we explore the universality of the three-body parameter by analyzing a number of model potentials [see $v_{\rm sch}$, v_λ^a, v_λ^b, $v_{\rm vdW}^{\rm hs}$ in Eqs. (S.1)-(S.4) of Ref. [26]] with different numbers of bound states.

Figure 1 (a) shows the adiabatic potentials U_ν at $|a|=\infty$ obtained using only the two-body Lennard-Jones potential, v_λ^a, supporting 25 dimer bound states. At first glance, it is difficult to identify any universal properties of these potentials. Efimov physics, however, occurs at a very small energy scale near the three-body breakup threshold. Indeed, a closer analysis of the energy range $|E|<\hbar^2/mr_{\rm vdW}^2$ [Fig. 1 (b)] reveals the universal properties of the key potential curve controlling Efimov states and universal scattering properties.

Figure 1(b) shows one of our most important pieces of theoretical evidence for universality of the three-body parameter: the effective adiabatic potentials W_ν obtained using v_λ^a for more and more two-body bound states converge to a single universal curve. [In some cases in

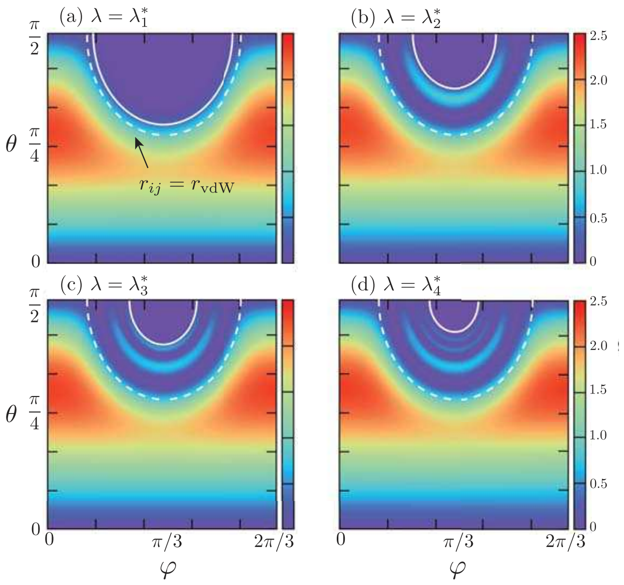

FIG. 2: Density plot of the three-body probability density $|\Phi_\nu(R;\theta,\varphi)|^2\sin 2\theta$ which determines the three particle configuration [see Fig. 1 (c)] in the θ-φ hyperangular plane for a fixed R ($\sin 2\theta$ is the volume element). (a)–(d) show the results for an R near the minimum of the Efimov potentials in Fig. 1 (b) for the first four poles of the v_λ^a model as indicated. (a) shows that there is a negligible probability to find the particles at distances smaller than $r_{\rm vdW}$ (outer dashed circle) and, of course, inside the $1/r^{12}$ repulsive barrier (inner solid circle). For higher poles, i.e., as the strength of the hard-core part of v_λ^a potential decreases, the potential becomes deeper and penetration into the region $r<r_{\rm vdW}$ is now classically allowed. Nevertheless, (b)–(e) show that inside-the-well suppression still efficiently prevents the particles from being found at distances $r<r_{\rm vdW}$. In fact, we calculated the probability to find the atoms at $r<r_{\rm vdW}$ and found to be in the range 2%–4%.

Fig. 1 (b) we have manually diabatized W_ν near sharp avoided crossings in order to improve the visualization (see Section D in Ref. [26]).] As one would expect, the usual Efimov behavior for the effective potentials, $W_\nu{=}-\hbar^2(s_0^2+1/4)/2\mu R^2$ with $s_0\approx 1.00624$, is recovered for $R>10r_{\rm vdW}$. It is remarkable, however, that W_ν also converge to a universal potential for $R<10r_{\rm vdW}$ and, more importantly, these effective potentials display a repulsive wall or barrier at $R\approx 2r_{\rm vdW}$. This barrier prevents the close collisions that would probe the short-range three-body physics, including three-body forces known to be important in chemistry, thus making the three-body parameter universal as we will confirm below. This is in fact our most striking result: *a sharp cliff or attraction in the two-body interactions produces a strongly repulsive universal barrier in the effective three-body interaction potential.*

Qualitatively, this universality derives from the reduced probability to find particles inside the attractive two-body potential well. This effect can be seen in terms of the channel functions Φ_ν (see Section C in Ref. [26]), in Figs. 1 (c)-(e) and the hyperangular probability densities in Fig. 2. In the adiabatic hyperspherical representation, the space forbidden to the particles fills an increasingly larger portion of the hyperangular volume as R decreases. This evolution can be visualized as the dashed lines in Fig. 2 (a)–(d) expanding outward. In the process, the channel function Φ_ν is squeezed into an increasingly smaller volume, driving its kinetic energy higher and producing the repulsive barrier in the universal Efimov potential. Moreover, this suppression implies that the details of the interaction should be largely unimportant. Consequently, different two-body model potentials should give similar three-body potentials. Figure 3 demonstrates this universality by comparing W_ν obtained from different potential models supporting many bound states. Perhaps more importantly, it compares them with the results obtained from the two-body model $v_{\rm vdW}^{\rm hs}$ that replaces the deep well by a hard wall, essentially eliminating the probability of observing any pair of atoms at short distances. *Quantitatively*, however, the fact that the barrier occurs only at $R\approx 2r_{\rm vdW}$ indicates that universality might not be as robust as in the cases discussed in Refs. [22–25]. It is thus important to quantify the value of the three-body parameter to assess the size of nonuniversal effects.

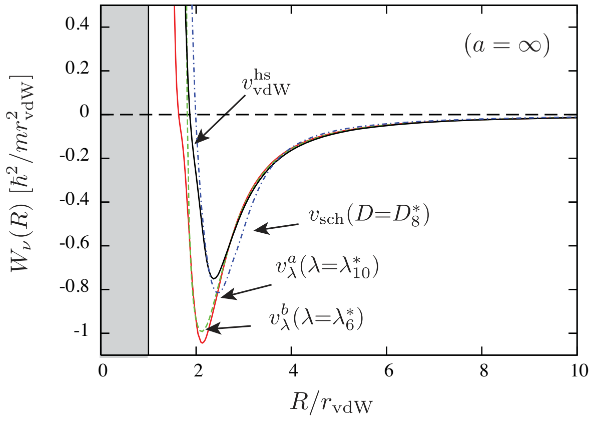

FIG. 3: The Efimov potential obtained from the different two-body potential models used here. The reasonably good agreement between the results obtained using models supporting many bound states ($v_{\rm sch}$, v_λ^a and v_λ^b) and $v_{\rm vdW}^{\rm hs}$ [obtained by replacing the deep potential well with a hard wall but having only *one* (zero-energy) bound state] supports our conclusion that the inside-the-well suppression of the wave function is the main physical mechanism behind the universality of the three-body effective potentials. The differences between these potentials are shown to lead to differences of a few percent in the three-body parameter. Note that the two-body potentials v_λ^a, v_λ^b, and $v_{\rm vdW}^{\rm hs}$ all have an asymptotic van der Waals tail, whereas $v_{\rm sch}$ decays exponentially at large distances.

In principle, the three-body parameter could be defined in terms of *any* observable related to the Efimov physics [15]. Two of its possible definitions are [15]: the value of $a=a_{\rm 3b}^-<0$ at which the first Efimov resonance

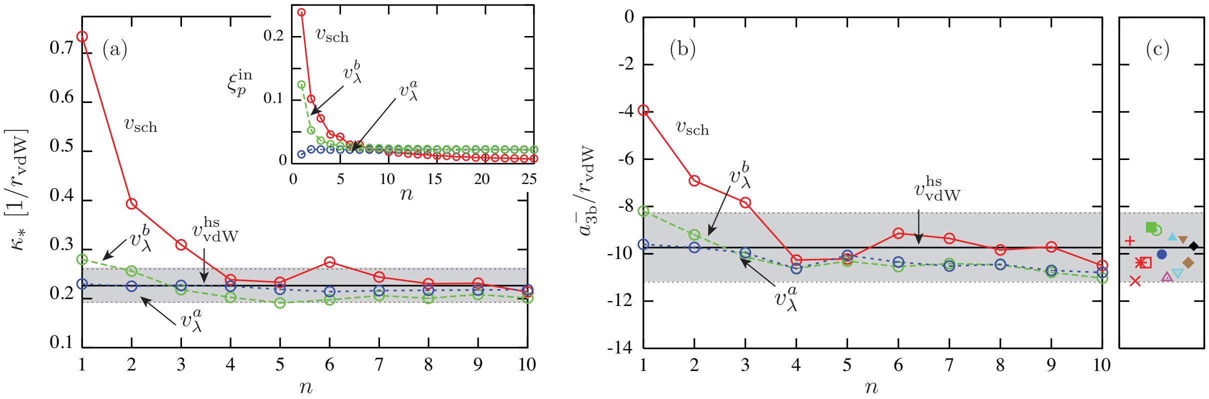

FIG. 4: Values for the three-body parameter (a) κ_* and (b) a_{3b}^- as functions of the number n of two-body s-wave bound states for each of the potential model studied here. The values for a_{3b}^- were obtained by determining the value of a at which the Efimov state becomes unbound. (c) Experimental values for a_{3b}^- for ^{133}Cs [3] (red: ×, +, □, and ∗), ^{39}K [4] (magenta: △), ^{7}Li [5] (blue: •) and [6, 7] (green: ■ and ○), ^{6}Li [8, 9] (cyan: ▲ and ▽) and [10, 11] (brown: ▼ and ◇), and ^{85}Rb [12] (black: ◆). The gray region specifies a band where there is a ±15% deviation from the $v_{\rm vdW}^{\rm hs}$ results. The inset of (a) shows the suppression parameter $\xi_p^{\rm in}$ [Eq. (S.5) in Ref. [26]] which can be roughly understood as the degree of sensitivity to nonuniversal corrections. Since $\xi_p^{\rm in}$ is always finite — even in the large n limit — nonuniversal effects associated with the details of the short-range interactions can still play an important role. One example is the large deviation in κ_* found for the $v_{\rm sch}$ ($n = 6$) model, caused by a weakly bound g-wave state. For $n > 10$ we expect κ_* and a_{3b}^- to lie within the range of ±15% stablished for $n \leq 10$.

appears in three-body recombination (see for instance Ref. [30]) and $\kappa_* = (m|E_{3b}^0|/\hbar^2)^{1/2}$, where E_{3b}^0 is the energy of the lowest Efimov state at $|a| \to \infty$. Our numerical results for κ_* and a_{3b}^- are shown in Figs. 4(a) and (b), respectively, demonstrating their universality in the limit of many bound states. In fact, the values for κ_* and a_{3b}^- in this limit differ by no more than 15% from the $v_{\rm vdW}^{\rm hs}$ results — $\kappa_* = 0.226(2)/r_{\rm vdW}$ and $a_{3b}^- = -9.73(3)r_{\rm vdW}$ [solid black line in Fig. 4(a) and (b)] — indicating, once again, that the universality of the three-body parameter is dependent upon the suppression of the probability density within the two-body potential wells. We note that our results for single channel two-body models should be applied for broad Feshbach resonances. Given this picture, we attribute the non-monotonic behavior of κ_* and a_{3b}^- in Fig. 4 to the small, but finite, probability to reach short distances, thus introducing nonuniversal effects related to the details of two- and three-body forces including interactions with an isolated perturbing channel. Nevertheless, our results for a_{3b}^- are consistent with the experimentally measured value for ^{133}Cs [2, 3], ^{39}K [4], ^{7}Li [5–7], ^{6}Li [8–11, 31], and ^{85}Rb [12], all of which lie within about 15% of the $v_{\rm vdW}^{\rm hs}$ result. Curiously, if one simply averages the experimental values, then the result differs from the $v_{\rm vdW}^{\rm hs}$ result by less than 3%.

Previous treatments have failed to predict the universality of the three-body parameter for various reasons. In treatments using zero-range interactions, for instance, the three-body parameter enters as a free parameter to cure the Thomas collapse [32], preventing any statement about its universality. Finite range models, like those used in some of our own treatments [18] [corresponding to the results for $v_{\rm sch}$ with $n = 2$ and 3 in Figs. 4 (a) and (b)], have failed for lack of substantial suppression of the probability density in the two-body wells. This scenario, however, should reflect better the situation for light nuclei having few bound states and shallow attraction. In contrast to Ref. [18], other models [24, 33–38] have found better agreement with experiments. Our analysis of these treatments, however, indicates that the two-body models used have many of the characteristics of our $v_{\rm vdW}^{\rm hs}$, therefore satisfying the prerequisite for a universal three-body parameter. A recent attempt [39] to explain the universality of the three-body parameter avoided explicit two-body models altogether, using instead an *ad hoc* hyperradial potential that bore little resemblance to our numerical potentials in Fig. 1. This *ad hoc* three-body potential displayed strong attraction at short distances in contrast to our key finding, that a cliff of attraction for two bodies produces a universal *repulsive* barrier in the three-body system. Consequently, even though a universal three-body parameter was found in Ref. [39], the fundamental understanding provided by the approach is uncertain (see our discussion in Section D of Ref. [26]).

In summary, our theoretical examination shows that the three-body parameter controlling many of the universal properties of Efimov physics can be a universal parameter under certain circumstances that should be realized in most ultracold neutral atom experiments. Provided the underlying two-body short-range interaction supports a large number of bound states, or it has some other property leading to the suppression of the wave function at short distances, three-body properties associated with Efimov physics can be expected to be universal. While these arguments suggest universality also for the three-body parameter in heteronuclear systems that exhibit Efimov physics with only resonant interspecies two-body interactions, verifying this prediction is a high priority for future theory and experiment. Equally important is the exploration of the relationship between $a < 0$ and $a > 0$ Efimov features — currently a subject of a number of controversies [3] — under the new perpective our present work offers.

Acknowledgments

The authors acknowledge stimulating discussions with Y. Wang, S. Jochim, M. Weidemüller, P. S. Julienne, and J. M. Hutson. We appreciate C. Chin communicating his ideas prior to publication and for useful comments on our manuscript. This work was supported by the U.S. National Science Foundation and by an AFOSR-MURI grant.

[1] V. Efimov, *Yad. Fiz.* **12**, 1080 (1970); Sov. J. Nucl. Phys. **12**, 589 (1971).
[2] T. Kraemer, *et al.*, Nature **440**, 315 (2006).
[3] M. Berninger, *et al.*, Phys. Rev. Lett. **107**, 120401 (2011).
[4] M. Zaccanti, *et al.*, Nature Phys. **5**, 586 (2009). Here, we are speculating that the feature observed in this experiment at $a = -11.02$ a.u. might in fact be a three-body resonance, instead of a four-body resonance. The possibility of such a reassignment is by no means proven, of course, and can only be answered through additional experimental studies.
[5] S. E. Pollack, D. Dries and R. G. Hulet, Science **326**, 1683 (2009).
[6] N. Gross, Z. Shotan, S. Kokkelmans, and L. Khaykovich, Phys. Rev. Lett. **103**, 163202 (2009).
[7] N. Gross, Z. Shotan, S. Kokkelmans, and L. Khaykovich, Phys. Rev. Lett. **105**, 103203 (2010).
[8] T. B. Ottenstein, T. Lompe, M. Kohnen, A. N. Wenz, and S. Jochim, Phys. Rev. Lett. **101**, 203202 (2008).
[9] T. Lompe, *et al.*, Phys. Rev. Lett. **105**, 103201 (2010).
[10] J. H. Huckans, J. R. Williams, E. L. Hazlett, R. W. Stites and K. M. OHara, Phys. Rev. Lett. **102**, 165302 (2009).
[11] J. R. Williams, *et al*, Phys. Rev. Lett. **103**, 130404 (2009).
[12] J. R. Wild, P. Makotyn, J. M. Pino, E. A. Cornell, and D. S. Jin, arXiv:1112.0362 (2011).
[13] G. Barontini, *et al.*, Phys. Rev. Lett. **103**, 043201 (2009).
[14] S. Nakajima, M. Horikoshi, T. Mukaiyama, P. Naidon, and M. Ueda, Phys. Rev. Lett. **105**, 023201 (2010).
[15] E. Braaten and H.-W. Hammer, Phys. Rep. **428**, 259 (2006).
[16] P. Soldán, M. T. Cvitas, and J. M. Hutson, *Phys. Rev. A* **67**, 054702 (2003).
[17] E. Epelbaum, *et al.*, Phys. Rev. C **66**, 064001 (2002).
[18] J. P. D'Incao, C. H. Greene, and B. D. Esry, J. Phys. B **42**, 044016 (2009).
[19] C. Chin, R. Grimm, P. S. Julienne, and E. Tiesinga, Rev. Mod. Phys. **82**, 1225 (2010).
[20] The van der Waals length is defined as $r_{\rm vdW} \equiv (2\mu_{\rm 2b}C_6/\hbar^2)^{1/4}/2$ where C_6 is the van der Waals coefficient and the two-body reduced mass $\mu_{\rm 2b}$. Note also that in Ref [3] the results were quoted in terms of the mean scattering length $\bar{a} \approx 0.9556 r_{\rm vdW}$ as defined in Ref. [21].
[21] V. V. Flambaum, G. F. Gribakin, and C. Harabati, Phys. Rev. A **59**, 1998 (1999).
[22] Y. Wang, J. P. D'Incao, and C. H. Greene, Phys. Rev. Lett. **106**, 233201 (2011).
[23] D. S. Petrov, Phys. Rev. Lett. **93**, 143201 (2004).
[24] P. Massignan, and H. T. C. Stoof, Phys. Rev. A **78**, 030701 (2008).
[25] Y. Wang, J. P. D'Incao, and B. D. Esry, Phys. Rev. A **83**, 042710 (2011).
[26] Supplementary material. EPAPS Document No. XXX
[27] R. Côté, H. Friedrich, and J. Trost, Phys. Rev. A **56**, 1781 (1997).
[28] H. Suno, B. D. Esry, C. H. Greene, and J. P. Burke, Phys. Rev. A **65**, 042725 (2002).
[29] J. Wang, J. P. D'Incao, and C. H. Greene, Phys. Rev. A **84**, 052721 (2011).
[30] B. D. Esry, C. H. Greene, and J. P. Burke, Phys. Rev. Lett. **83**, 1751 (1999).
[31] For the experiments with ^{6}Li [8–11], we have determined $a^-_{\rm 3b}$ by using the definition of the mean scattering length from: Wenz, A. N. *et al.*, Phys. Rev. A **80**, 040702(R) (2009).
[32] L. H. Thomas, Phys. Rev. **47**, 903 (1935).
[33] P. Naidon, and M. Ueda, Comptes Rendus Physique **12**, 13 (2011).
[34] P. Naidon, E. Hiyama, M. Ueda, arXiv:1109.5807 (2011).
[35] S. Nakajima, M. Horikoshi, T. Mukaiyama, P. Naidon, and M. Ueda, Phys. Rev. Lett. **106**, 143201 (2011).
[36] M. D. Lee, T. Köhler, and P. S. Julienne, Phys. Rev. A **76**, 012720 (2007).
[37] M. Jona-Lasinio, and L. Pricoupenko, Phys. Rev. Lett. **104**, 023201 (2010).
[38] R. Schmidt, S. P. Rath, and W. Zwerger, arXiv:1201.4310 (2012).
[39] C. Chin, arXiv:1111.1484 (2011).

SUPPLEMENTARY MATERIAL

A. Two-body model interactions

Our theoretical model for the two-body interactions mimics the tunability of the interatomic interactions via Fano-Feshbach resonances [1] by directly altering the strength of the interparticle interactions and, consequently, leading to the desired changes in a. In this work, we have considered various model interactions in order to test the universality of our three-body calculations — we consider a result is universal if it is independent of the particular choice of the underlying two-body interaction. The models we have used for the two-body interactions are:

$$v_{\rm sch}(r) = -D{\rm sech}^2\left(r/r_0\right), \tag{S.1}$$

$$v_\lambda^a(r) = -\frac{C_6}{r^6}\left(1-\lambda^6/r^6\right), \tag{S.2}$$

$$v_\lambda^b(r) = -\frac{C_6}{r^6}\exp\left(-\lambda^6/r^6\right), \tag{S.3}$$

$$v_{\rm vdW}^{\rm hs}(r) = B_{\rm hs}\Theta\left(r_{\rm hs}-r\right) - \frac{C_6}{r^6}\Theta\left(r-r_{\rm hs}\right). \tag{S.4}$$

The potential model in Eq. (S.1) is the modified Pöschl-Teller potential, where D determines the potential depth; Eq. (S.2) is the usual Lennard-Jones potential; and Eq. (S.3) is a dispersion potential with a soft wall at short range. In Eq. (S.4), $\Theta(x)$ the step-function [$\Theta(x)=0$ for $x<0$ and 1 elsewhere. In practice, however, we have used a smooth representation of the step-function Θ in order to simplify our numerical calculations.] The potential in Eq. (S.4), therefore, consists of a hard-sphere potential for $r<r_{\rm hs}$ ($B_{\rm hs}\gg C_6/r_{\rm hs}^6$) and a long-range dispersion $-1/r^6$ potential for $r>r_{\rm hs}$. In the present study, the parameters D and λ in Eqs. (S.1)-(S.3) are adjusted to give the desired a and number of bound states. For convenience, we denote the values of D and λ at which there exist zero-energy bound states ($|a|\to\infty$) as D_n^* and λ_n^*, where n corresponds to the number of s-wave bound states. For the potential model in Eq. (S.4), however, we adjusted $r_{\rm hs}$ to produce the changes in a, but we only performed three-body calculations near the first pole at $r_{\rm hs}\approx 0.8828r_{\rm vdW}$.

The potential models in Eqs. (S.2)-(S.4) have in common the same large r behavior given by the van der Waals interaction, $-C_6/r^6$, with C_6 the van der Waals dispersion coefficient. For these potentials, the important length scale is the van der Waals length defined as $r_{\rm vdW}\equiv(2\mu_{\rm 2b}C_6/\hbar^2)^{1/4}/2$ [2], where $\mu_{\rm 2b}$ is two-body reduced mass. Therefore, in order to compare the results from these models to those for $v_{\rm sch}$, we define an equivalent $r_{\rm vdW}$ for $v_{\rm sch}$ through the relationship between $r_{\rm vdW}$ and the effective range $r_{\rm eff}$ for $v_{\rm sch}$, namely, $r_{\rm vdW}\approx r_{\rm eff}/2.78947$ [2], valid for values $|a|\gg r_0$. In fact, for $v_{\rm sch}$ we have found that $r_{\rm eff}(|a|=\infty)$ depends on the potential depth D_n^*, while for van der Waals type of interactions, such as those in Eqs. (S.2)-(S.4), $r_{\rm eff}$ is fixed by $r_{\rm eff}\approx 2.78947(2\mu_{\rm 2b}C_6/\hbar^2)^{1/4}/2$. Nevertheless, after rescaling the three-body results obtained from $v_{\rm sch}$ in terms of $r_{\rm vdW}$, we found good agreement with those obtained using v_λ^a, v_λ^b, and $v_{\rm vdW}^{\rm hs}$, thus indicating that the effective range is in fact the most relevant length scale in the problem. We chose, however, to keep our results in terms of $r_{\rm vdW}$ to make a closer analogy to the experiments using alkali atoms.

B. Suppression of inside-the-well probability

Our claim here is that the origin of the universality of the three-body parameter is related to the suppression of the probability to find two particles at distances $r<r_{\rm vdW}$. This suppression leads to the formation of the universal three-body potential barrier near $R\approx 2r_{\rm vdW}$, thus strongly suppressing the three-body wave function at shorter distances where the details of the two- and three-body interactions are important [see Fig. 1 (b) of our main text]. Next we explore the origin of this suppression at the two-body level.

To gain some insight into the likelihood of finding particles inside the potential well, we start by defining the following quantities,

$$\xi_p^{\rm in}(k) \;=\; \frac{1}{r_0}\int_0^{r_0}|\psi_k(r)|^2{\rm d}r, \tag{S.5}$$

$$\xi_p^{\rm out}(k) \;=\; \lim_{r\to\infty}\frac{1}{r-r_0}\int_{r_0}^{r}|\psi_k(r)|^2{\rm d}r, \tag{S.6}$$

where $\psi_k(r)$ is the two-body scattering wave function at energy $E_{\rm 2b}=k^2/2\mu_{\rm 2b}$, defined such that

$$\psi_k(r)\overset{r\to\infty}{=}\frac{\sin(kr+\delta)}{\sin\delta}, \tag{S.7}$$

with $\delta\equiv\delta(k)$ the s-wave scattering phase shift. This definition for $\psi_k(r)$, therefore, leads to a zero-energy ($k\to0$) wave function of the form: $\psi_0(r)=1-r/a$. [Note that in the above equations r_0 is the characteristic range of the two-body interaction. For the potential model in Eq. (S.1), r_0 is just the quantity in the argument of the sech function, while for the potential models in Eqs. (S.2)-(S.4) it is defined to be $r_0=r_{\rm vdW}$].

The parameters $\xi_p^{\rm in}$ and $\xi_p^{\rm out}$ can be associated with the "average" amplitude of the wave function inside and outside the potential well, respectively. We, therefore, define the amplitude inside the well *relative to the amplitude outside the well* as:

$$\xi_p^{\rm rel}(k) \;=\; \frac{\xi_p^{\rm in}(k)}{\xi_p^{\rm out}(k)} = 2\,\xi_p^{\rm in}(k)\sin^2\delta. \tag{S.8}$$

The relative amplitude above vanishes in the limit $k\to0$ ($\sin\delta\approx -ka$), as a result of our choice for the asymptotic solution in Eq. (S.7), except at $|a|=\infty$, when δ is an odd multiple of $\pi/2$. The quantity $\xi_p^{\rm in}(k)$, however, remains finite in the $k\to0$ limit. We believe, therefore, that $\xi_p^{\rm in}(k\to0)$ to be the most relevant parameter for our analysis on the inside-the-well suppression. Rigorously speaking, $\xi_p^{\rm in}$ is *not* a probability, but it does measure the likelihood of finding two particles within $r<r_0$, where the short-range interactions are experienced. Figure S.1 shows a typical result for $|a|/r_0$ and $\xi_p^{\rm in}(k\to0)$ for the two-body potential in Eq. (S.1). Figure S.1 shows that in the universal regime near the poles in a, the wavefunction is suppressed (small $\xi_p^{\rm in}$) and that this suppression becomes more efficient as the potential becomes deeper

and more states are bound. The black filled circles, open circles and open squares in Fig. S.1, showing the values of $\xi_p^{\rm in}$ at $|a| \to \infty$, $a = 5r_0$, and $a = -5r_0$, respectively, illustrate this trend. Note, however, that for values $|a| \lesssim r_0$, the parameter $\xi_p^{\rm in}$ quickly increases, indicating a higher likelihood to find particles inside the potential well. Similar results are also obtained for the potentials v_λ^a and v_λ^b [Eqs. (S.2) and (S.3), respectively].

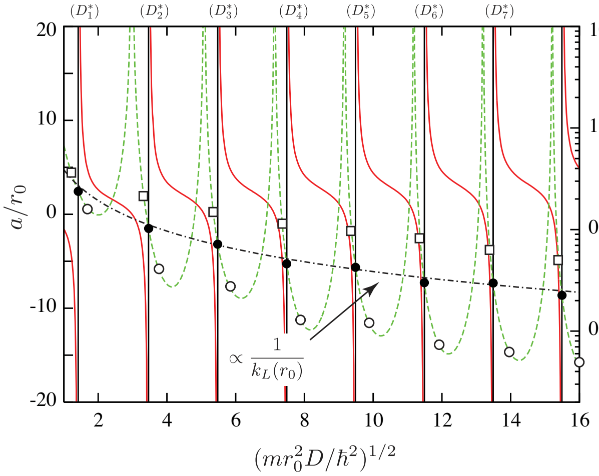

FIG. S.1: The red solid line represents the scattering length, a/r_0, while the green dashed lines represents the parameter $\xi_p^{\rm in}(k \to 0)$. Both quantities are given as a function of the depth D of the two-body interaction model $v_{\rm sch}$ [Eq. (S.1)], whose values for which $|a| = \infty$ are indicated in the figure as D_n^*, where n is the number of s-wave states. Black circles, open circles and open squares are the values of $\xi_p^{\rm in}$ at $|a| \to \infty$, $a = 5r_0$, and $a = -5r_0$, showing the suppression of the $\xi_p^{\rm in}$ as the number of bound states increases. The results for $\xi_p^{\rm in}$ also show higher efficiency of the inside-the-well suppression for $|a|/r_0 \gg 1$. The black dash-dotted line shows the semi-classical suppression factor $1/k_L(r_0)$ demonstrating the origin of the suppression mechanism.

The suppression in $\xi_p^{\rm in}$ (for a fixed value of $|a| \gg r_0$) can be understood to be a result of the usual semiclassical suppression of the wave function. In the WKB approach [3–5], the wave function inside the potential well can be written as,

$$\psi_{\rm WKB}(r < r_0) = \frac{C}{k_L^{1/2}(r)} \sin\left[\int^r k_L(r')dr' + \frac{\pi}{4}\right], \quad \text{(S.9)}$$

where C is a normalization constant and $k_L^2(r) = 2\mu_{\rm 2b}[E_{\rm 2b} - v(r)]$ defines the *local* wave number $k_L(r)$. Therefore, for deep potentials, the suppression of the wave function inside the potential well is simply related to factor $k_L(r)^{-1/2}$ which leads to the suppression of the amplitude of the WKB wave function [Eq. (S.9)] between r and $r+dr$. Physically, this can be seen as the increase of the *local* velocity $\hbar k_L(r)/m$ (m being the particle mass) and, therefore, the decrease of the time spent in that interval dr, $[\hbar k_L(r)/mdr]^{-1}$. Therefore, in the WKB approximation, one would expect $\xi_p^{\rm in}$ to be simply proportional to $1/k_L$. We test this expectation by plotting in Fig. S.1 the value of $1/k_L(r_0)$ (black dash-dotted line) which shows that the suppression in $\xi_p^{\rm in}(k \to 0)$ is consistent with the semiclassical suppression described above.

We have also considered the possibility that two-body quantum reflection [6, 7] could be responsible for the suppression of inside-the-well probability, and consequently the universality of the three-body parameter. Quantum reflection is a fundamental phenomenon involving reflection of a low energy quantum matter wave from a potential *cliff*. In the context of ultracold collisions of ground state neutral atoms, quantum reflection can occur when two atoms approach within a distance comparable to the range of the interaction, r_0, and it is caused by the rapid change of the potential in this region [7]. In that case, just a fraction of the incoming wave probes the details of the atom-atom interaction at $r < r_0$. Nevertheless, our analysis leads us to believe that this is of secondary importance. The main reason is that in a three-body system, even at zero (three-body) energy, two particles can have energies that are not low enough to ensure that quantum reflection plays a rule. In fact, accordingly to our estimates, in a three-body system the average two-body energy will be proportional to $1/2\mu R^2$. This implies that near the universal barrier ($R \approx 2r_{\rm vdW}$) the two-body energy can be of the order of $1/mr_{\rm vdW}^2$. Based on a model similar to the one used in Ref. [7] the reflection probability at such energies is about 10%, which is too low to explain our observations. Our above analysis, however, shows that for such energies $\xi_p^{\rm in}(k)$ does not differs substantially from $\xi_p^{\rm in}(0)$, offering a more consistent picture than quantum reflection. Evidently, to precisely quantify the importance of quantum reflection requires a much more detailed analysis of how the energy of two particles in a three-body system behaves as a function of R, which is beyond the scope of our present study.

C. Three-body hyperspherical adiabatic representation

As mentioned in our main text, our analysis of the universality of the three-body parameter was based on the hyperspherical adiabatic representation. The following, is a sketch of its basic aspects and fundamental equations. A more detailed description can be found, for instance, in Refs. [8, 9]. We start here from the hyperradial Schrödinger equation :

$$\left[-\frac{\hbar^2}{2\mu}\frac{d^2}{dR^2} + W_\nu(R)\right]F_\nu(R) + \sum_{\nu' \neq \nu} W_{\nu\nu'}(R)F_{\nu'}(R) = EF_\nu(R). \quad \text{(S.10)}$$

The hyperradius R can be expressed in terms of interparticle distances for a system of three equal masses m, $R = 3^{-1/4}(r_{12}^2 + r_{23}^2 + r_{31}^2)^{1/2}$, and describes the overall size of the system; ν is a collective index that represents all quantum numbers necessary to label each channel; $\mu = m/\sqrt{3}$ is the three-body reduced mass; E is the total energy; and F_ν is the hyperradial wave function. The simple picture resulting from this representation originates from the fact that nonadiabatic couplings $W_{\nu\nu'}$ are the quantities that drive inelastic transitions, and that the effective hyperradial potentials W_ν, like any usual potential, support bound and resonant states, but now for the three particle system.

To obtain W_ν and $W_{\nu\nu'}$, however, one needs to diagonalize the adiabatic Hamiltonian $H_{\rm ad}$ which includes the hyperangular kinetic energy and *all* of the interactions [8, 9]. Our present study has assumed that the interactions are given as a pairwise sum of two-body model potentials and used those from Eqs. (S.1)-(S.4). The eigenvalues of $H_{\rm ad}$, determined for fixed values of R by using the method in Ref. [9], are the three-body potentials $U_\nu(R)$ [main text Fig. 1 (a)] associated to the respective channel functions (eigenfunctions) $\Phi_\nu(R;\Omega)$ [10, 11]. Therefore, the channel functions Φ_ν contain all the information necessary to determine, for fixed values of R, the geometric structure of the three particle system. For our present study concerning three identical bosons in the total angular momentum state $J^\pi = 0^+$ (π being the parity), the set of hyperangles Ω [9] is reduced to simply $\{\theta, \varphi\}$. This helps to visualize the geometric structure of the three-body system [see Figs. 1 (c)-(e) and Fig. 2 of our main text].

Finally, to determine the effective potentials W_ν and nonadiabatic couplings $W_{\nu\nu'}$, which are the main quantities in Eq. (S.10), one can use the expressions,

$$W_\nu(R) = U_\nu(R) - \frac{\hbar^2}{2\mu}Q_{\nu\nu}(R), \tag{S.11}$$

$$W_{\nu\nu'}(R) = -\frac{\hbar^2}{2\mu}\left[2P_{\nu\nu'}(R)\frac{d}{dR} + Q_{\nu\nu'}(R)\right], \tag{S.12}$$

where

$$P_{\nu\nu'}(R) = \langle\!\langle\Phi_\nu(R;\Omega)|\frac{\partial}{\partial R}|\Phi_{\nu'}(R;\Omega)\rangle\!\rangle, \tag{S.13}$$

$$Q_{\nu\nu'}(R) = \langle\!\langle\Phi_\nu(R;\Omega)|\frac{\partial^2}{\partial R^2}|\Phi_{\nu'}(R;\Omega)\rangle\!\rangle. \tag{S.14}$$

In the above expressions, the double-bracket matrix elements indicate that integrations are carried out over only the hyperangles Ω. As is mentioned in the main text, to treat problems with deep two-body potentials, and consequently many bound states, we have used a modified version of the above formulation since $P_{\nu\nu'}$ and $Q_{\nu\nu'}$, defined above, can become numerically unstable. This problem can be overcome using the formulation developed in Ref. [12]. Apart from this more technical aspect, the above formulation gives the general ideas concerning the hyperspherical representation. We encourage the interested reader to look for more details in Refs. [8, 9, 12].

D. Effective adiabatic potentials

The effective potentials shown in Fig. 1 (a) of the main text are very complicated, making identification of the important physics challenging. For that reason, this section presents some details of our work that not only give support to our physical interpretation of the nature of the three-body parameter but also show how some important nonuniversal aspects appear in the hyperspherical adiabatic representation. In fact, Fig. S.2 shows some of the most drastic nonadiabatic effects found in our calculations. The model proposed in Ref. [14] is also considered, and we show that this model offers an interesting qualitative picture; but since incorporation of corrections to that model diminishes its accuracy in the three-body parameter universality, its agreement with experiment might be fortuitous.

We first consider the validity of the single-channel adiabatic hyperspherical approximation and point out the manner in which some important nonuniversal features manifest themselves. Figure S.2 shows the results for $U_\nu(R)$ and $W_\nu(R)$ obtained from three different two-body potential models. Figures S.2 (a) and (b) show the results for the potential models $v_\lambda^a(\lambda = \lambda_2^*)$ and $v_\lambda^a(\lambda = \lambda_{10}^*)$ [Eq. (S.2)], respectively, while Fig. S.2 (c) shows the results obtained for $v_{\rm sch}(D = D_6^*)$ [Eq. (S.1)]. The most striking aspect of these figures is that $U_\nu(R)$ and $W_\nu(R)$ are substantially different, meaning that the nonadiabatic couplings $P_{\nu\nu'}(R)$ and $Q_{\nu\nu'}(R)$ [Eqs. (S.13) and (S.14)] are important near $R = r_{\rm vdW}$. Therefore, it is clear that one needs to go beyond a single channel approximation in order to describe the three-body observables. It is worth noting that the nonadiabatic couplings originate from the hyperradial kinetic energy. Their large values are thus consistent with our physical picture in which the *local* kinetic energy increases and generates the repulsive barrier in our effective potentials. It is also worth mentioning that since the three-body repulsive barrier prevents particles from approaching to small distances, the question of whether or not the short range physics actually changes as a function of the external magnetic field (as in experiments in ultracold quantum gases) [13] can not be directly answered by observing features related to Efimov physics.

The strong multichannel nature of the problem can be illustrated by comparing the results obtained from a single channel approximation to Eq. (S.10), i.e., $W_{\nu\nu'}(R) = 0$ $(\nu \neq \nu')$, with our solutions of the fully coupled system of equations. Figure S.3 (a) shows the three-body parameter κ_* [related to the energy of the lowest Efimov state through the relation $\kappa_* = (mE/\hbar^2)^{1/2}$] obtained for the v_λ^a model obtained in the single channel approximation (open triangles) as well as our full numerical results (open circles). The disagreement between these quantities increases with the number of s-wave bound states n, meaning that the physics controlling the results becomes more and more multichannel in nature. Nevertheless, we find that by imposing a simple change in the adiabatic

(a) $v_\lambda^a(\lambda = \lambda_2^*)$

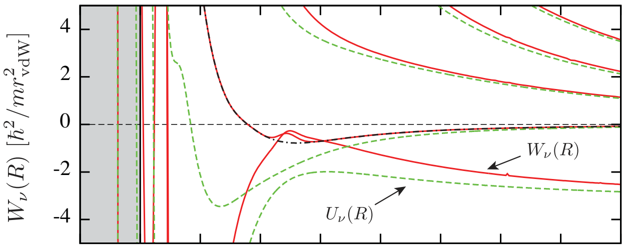

(b) $v_\lambda^a(\lambda = \lambda_{10}^*)$

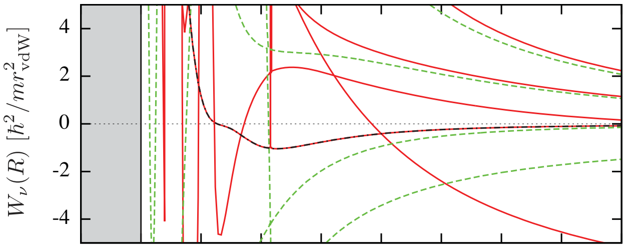

(c) $v_{\rm sch}(D = D_6^*)$

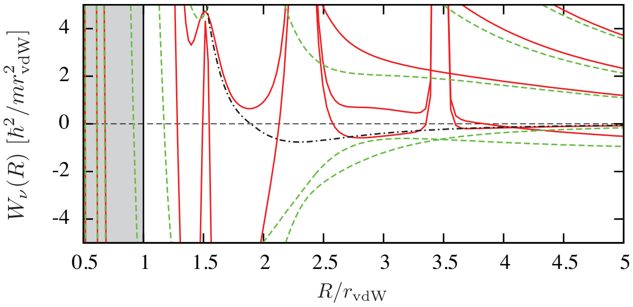

FIG. S.2: Comparison of $U_\nu(R)$ (green dashed curves) and $W_\nu(R)$ (red solid curves) demonstrating the importance of nonadiabatic effects introduced by $Q_{\nu\nu}(R)$ in Eq. (S.11). (a) and (b) show the results for the potential models $v_\lambda^a(\lambda = \lambda_2^*)$ and $v_\lambda^a(\lambda = \lambda_{10}^*)$ [Eq. (S.2)], respectively, and in (c) we show the results obtained for $v_{\rm sch}(D = D_6^*)$ [Eq. (S.1)]. (a) and (b) also show the effect of the diabatization scheme used in order to prepare some of our figures in the main text (dash-dotted curves). The goal of the diabatization is to eliminate the sharp features resulting from $Q_{\nu\nu}(R)$ in Eq. (S.11) which should not contribute substantially to the three-body observables. The case shown in (c), however, does not allow us to easily trace the diabatic version of the potentials W_ν. In this case, however, the "less" sharp features have a larger contribution due to the crossing with a three-body channel describing a collision between a g-wave molecular state and a free atom, giving rise to the anomalous $n = 6$ point for the $v_{\rm sch}$ model in Fig. 4 of the main text. Although such cases are relatively infrequent in our calculations (and occur mostly for the $v_{\rm sch}$ model), they do illustrate nonuniversal effects that can affect the three-body parameter. Nevertheless, the three-body observables obtained for cases like the one shown in (c) are still within the 15% range we claimed for the universality of the three-body parameter.

potentials near the barrier — to make the barrier *more* repulsive [see Fig. S.3 (b)] — the single channel approximation for κ_* [filled circles in Fig. S.3 (a)] reproduces the full numerical calculations much better. This agreement indicates that most of the nonadiabaticity of the problem is related to the exact shape of the barrier and that, to some extent, the effect of the nonadiabatic couplings is to make the effective potential W_ν more repulsive. For these reasons and, of course, the universality of our full calculations (see for instance Fig. 4 of our main text), we believe that the short-range barrier in the three-body effective potentials indeed offers a physically valid explanation of the universality of the three-body parameter. We emphasize, though, that Fig. 4 in the main text only includes the results from our essentially exact solutions of the full calculations. The single channel results discussed here are intended only as support of our physical interpretation.

It is within this context that we analyzed the model proposed in Ref. [14]. In Ref. [14], the three-body effective potential important for Efimov physics was estimated by considering the different aspects controlling the physics at small and large distances. At distances comparable to $R = r_{\rm vdW}$, it was assumed that the effective three-body potential is dominated by the contributions from equilateral triangle geometries and included only on two-body interactions. Under these assumptions, $r_{12} = r_{23} = r_{31} = r$ giving $R = 3^{1/4}r$ (note that our definition for R differs from that used in Ref. [14]), the effective potential can be written as

$$\begin{aligned} V_m(R) &= -C_6/r_{12}^6 - C_6/r_{23}^6 - C_6/r_{31}^6 \\ &= -3C_6/r^6 = -3 \times 3^{3/2} C_6/R^6. \quad \text{(S.15)} \end{aligned}$$

This potential is expected to be valid for distances $R < \bar{A} = 4\pi\Gamma(1/4)^{-2}3^{1/4}3^{3/8}r_{\rm vdW} \approx 1.9r_{\rm vdW}$ [2]. With our method, however, we have the means to check the validity of Eq. (S.15) by comparing it with our numerically calculated potentials. Figure S.4 shows the three-body potentials obtained using the $v_\lambda^a(\lambda = \lambda_{10}^*)$ model supporting a total of 100 two-body bound states. The potential from Eq. (S.15) is the black solid line passing near the series of avoided crossings and might be loosely viewed as diabatically connecting the fully numerical potentials. This relation is reasonable given that this sequence of avoided crossings has been shown in Ref. [15] to be related to the transition of the system from an equilateral triangle geometry to other geometries. This figure therefore suggests that approximating the short range physics by Eq. (S.15) is not wholly unphysical, but its validity depends on a strong assumption of diabaticity through a large number of avoided crossings and is thus probably *not* an approximation satisfactory for a more quantitative analysis.

The potential in Eq. (S.15), however, was not actually used in the calculations in Ref. [14]. Instead, it was used to motivate a claim that three-body quantum reflection plays an important role, allowing the short range behavior to be replaced by a repulsive potential for distances

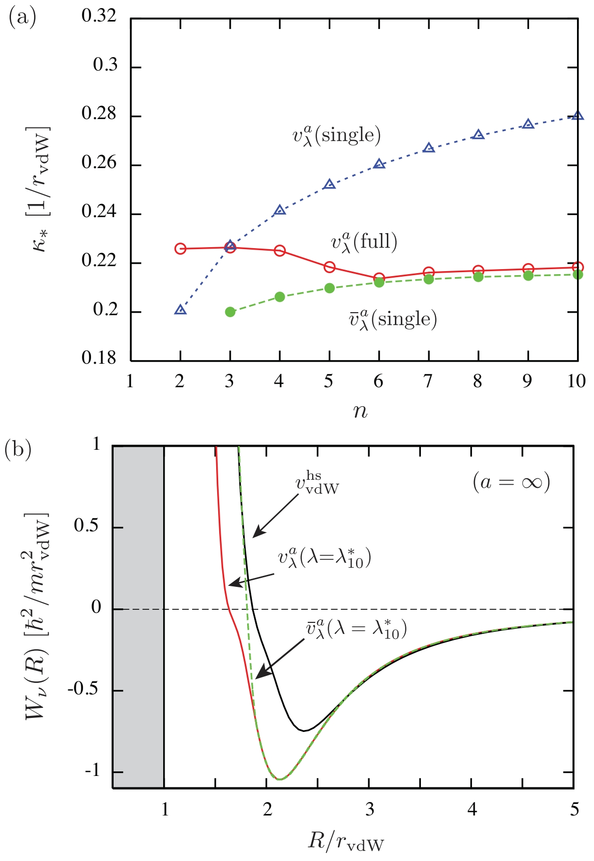

FIG. S.3: (a) This figure compares the energies (as characterized by the three-body parameter κ_*) obtained from a single channel approximation with our full calculations. The three-body parameter κ_* is shown for the v^a_λ model in the single channel approximation (open triangles) as well as for our full numerical results (open circles). The single channel approximation can be improved by imposing a simple change in the adiabatic potentials near the barrier, as is shown in (b). There we smoothly connect the potential for v^a_λ (red solid line) to the barrier obtained for $v^{hs}_{\rm vdW}$ (black solid line), resulting in the potential labeled by $\bar{v}^a_\lambda$ (green solid line). This new potential is actually more repulsive and has energies [filled circles in (a)] that are much closer to our full numerical calculations.

$R < \bar{A} \approx 1.9 r_{\rm vdW}$. It is interesting to note that the value $R \approx 1.9 r_{\rm vdW}$ obtained from Ref. [14] for the position of the hard wall is quite close to the hyperradius where our potentials exhibit the universal barrier (see Fig. S.2, for instance), indicating that $\bar{A}$ might have some physical meaning. It is worth mentioning, however, that the barrier we observed in our calculations is model independent, i.e., it doesn't rely on the particular model used for the two-body interaction. For distances $R > \bar{A}$, the model in Ref. [14] assumed the three-body effective potentials to be given by the universal Efimov formula,

$$V_E(R) \;=\; -\hbar^2\frac{s_0^2+1/4}{2\mu R^2}. \qquad \text{(S.16)}$$

It is well known [27], however, that this potential is valid for $r_{\rm vdW} \ll R \ll |a|$, and $R = 1.9 r_{\rm vdW}$ is certainly out of this range. In fact, one can see in Fig. 1 (b) of the main text, that the use of the Efimov potential [Eq. (S.16)] for $R < 10 r_{\rm vdW}$ is a crude approximation. Nevertheless, using this model, Ref. [14] obtains $a^-_{3\rm b} \approx -9.48 r_{\rm vdW}$, a value consistent with experiments [16–26] as well as with our present calculations for $a^-_{3\rm b}$. However, extending the model of Ref. [14] to the limit $|a| = \infty$, we obtained $\kappa_* \approx 0.037/r_{\rm vdW}$. Our result, by way of contrast, using $v^{\rm hs}_{\rm vdW}$ [Eq. (S.4)] is $\kappa_* = 0.226(2)/r_{\rm vdW}$. We also have tested the effects of finite a corrections on the model of Ref. [14] by replacing Eq. (S.16) with the three-body potential obtained with a zero-range model of the two-body interactions [28]. These corrections are particularly important near $R = |a|$. With this modification, the model of Ref. [14] leads to $a^-_{3\rm b} \approx -39.96 r_{\rm vdW}$. For these reasons, we believe that this model's agreement with our results and experimental data is fortuitous.

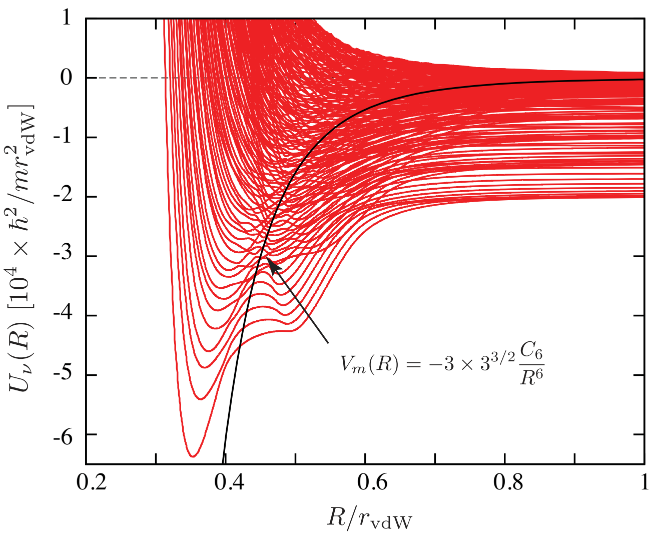

FIG. S.4: This figure shows the three-body potentials obtained using the $v^a_\lambda(\lambda = \lambda^*_{10})$ model supporting a total of 100 bound states. Roughly speaking, the potential of Eq. (S.15) [14] (black solid line) can be seen as a diabatic potential since it passes near one of the series of avoided crossings.

While multichannel couplings are needed to quantitatively describe this system, it is possible to construct an effective hyperradial potential curve that correctly describes the behavior of three atoms in the universal regime. Such a potential curve could be useful for simplified future studies. The approximate form obtained from the present study is:

$$\begin{aligned}\frac{2\mu r^2_{\rm vdW}}{\hbar^2}W^u_\nu(R) \approx &-\frac{s_0^2+1/4}{(R/r_{\rm vdW})^2}\\ &-\frac{2.334}{(R/r_{\rm vdW})^3}-\frac{1.348}{(R/r_{\rm vdW})^4}\\ &-\frac{44.52}{(R/r_{\rm vdW})^5}+\frac{4.0\times10^4}{(R/r_{\rm vdW})^{16}}. \qquad \text{(S.17)}\end{aligned}$$

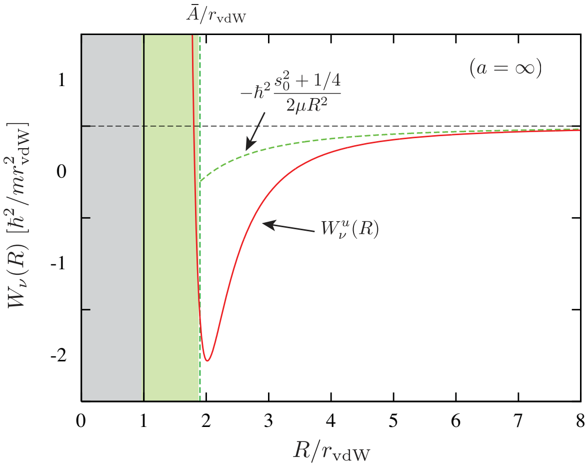

FIG. S.5: Comparison between the effective potential obtained from Ref. [14] and the potential from Eq. (S.17).

Here μ is the three-body reduced mass and r_{vdW} is the two-body van der Waals length. For comparison the speculative potential curve proposed by Chin [14] is shown, which does not resemble the present result even qualitatively at small distances, as it exhibits far too little attraction in the region $R = 2 - 5r_{\rm vdW}$.

---

[1] C. Chin, R. Grimm, P. S. Julienne, and E. Tiesinga, Rev. Mod. Phys. **82**, 1225 (2010).

[2] V. V. Flambaum, G. F. Gribakin, and C. Harabati, Phys. Rev. A **59**, 1998 (1999).

[3] G. F. Gribakin and V. V. Flambaum, Phys. Rev. A **48**, 546 (1993).

[4] M. Aymar, C. H. Greene, and E. Luc-Koenig, Rev. Mod. Phys. **68**, 1015 (1996).

[5] M. V. Berry and K. Mount, Rep. Prog. Phys. **35**, 315 (1972).

[6] G. L. Klimchitskaya, U. Mohideen, and V. M. Mostepanenko, Rev. Mod. Phys. **81**, 1827 (2009).

[7] R. Côté, H. Friedrich, and J. Trost, Phys. Rev. A **56**, 1781 (1997).

[8] J. P. D'Incao, C. H. Greene, and B. D. Esry, J. Phys. B **42**, 044016 (2009).

[9] H. Suno, B. D. Esry, C. H. Greene, and Burke, Phys. Rev. A **65**, 042725 (2002).

[10] J. P. D'Incao, S. C. Cheng, H. Suno, and B. D. Esry, Phys. Rev. A **75**, 032503 (2007).

[11] V. Kokoouline and C. H. Greene, Phys. Rev. A **68**, 012703 (2003).

[12] J. Wang, J. P. D'Incao, and C. H. Greene, Phys. Rev. A **84**, 052721 (2011).

[13] N. Gemelke, C.-L. Hung, C.-L., X. Zhang, and C. Chin, arXiv:0812.1317 (2008).

[14] C. Chin, arXiv:1111.1484 (2011).

[15] D. Blume, C. H. Greene, and B. D. Esry, J. Chem. Phys. **113**, 2145 (2000).

[16] T. Kraemer, *et al.*, Nature **440**, 315 (2006).

[17] M. Berninger, *et al.*, Phys. Rev. Lett. **107**, 120401 (2011).

[18] M. Zaccanti, *et al.*, Nature Phys. **5**, 586 (2009). Here, we are speculating that the feature observed in this experiment at $a = -11.02$ a.u. might in fact be a three-body resonance, instead of a four-body resonance. The possibility of such a reassignment is by no means proven, of course, and can only be answered through additional experimental studies.

[19] S. E. Pollack, D. Dries and R. G. Hulet, Science **326**, 1683 (2009).

[20] N. Gross, Z. Shotan, S. Kokkelmans, and L. Khaykovich, Phys. Rev. Lett. **103**, 163202 (2009).

[21] N. Gross, Z. Shotan, S. Kokkelmans, and L. Khaykovich, Phys. Rev. Lett. **105**, 103203 (2010).

[22] T. B. Ottenstein, T. Lompe, M. Kohnen, A. N. Wenz, and S. Jochim, Phys. Rev. Lett. **101**, 203202 (2008).

[23] T. Lompe, *et al.*, Phys. Rev. Lett. **105**, 103201 (2010).

[24] J. H. Huckans, J. R. Williams, E. L. Hazlett, R. W. Stites and K. M. OHara, Phys. Rev. Lett. **102**, 165302 (2009).

[25] J. R. Williams, *et al*, Phys. Rev. Lett. **103**, 130404 (2009).

[26] J. R. Wild, P. Makotyn, J. M. Pino, E. A. Cornell, and D. S. Jin, arXiv:1112.0362 (2011).

[27] V. Efimov, Yad. Fiz. **12**, 1080 (1970); Sov. J. Nucl. Phys. **12**, 589 (1971).

[28] S. T. Rittenhouse, N. P. Mehta, and C. H. Greene, Phys. Rev. A **82** , 022706 (2010).